Exploring the quantum chromodynamics phase diagram: from HAdrons and NUClei to MATter under extreme conditions (HADNUCMAT)

Toward Improved Nuclear Energy Density Functionals

Mengying QIU (丘梦莹)

Sun Yat-sen University & University of Barcelona

Collaboration
Xavier Roca-Maza (University of Barcelona & University of Milan) ;
Zhen Zhang (Sun Yat-sen University);
Liewen Chen, Tonggang Yue (Shanghai Jiao Tong university)

Nuclear Energy Density Functional

- Approximations/theory to describe nuclear properties

Ab initio approaches	Configuration interaction approach	Nuclear energy density functionals (EDF)
		applied to almost all nuclei (phenomenological)

- Paths toward constructing phenomenological nuclear energy density functionals

✓ Start from an **effective nuclear interaction or Lagrangian** : $\hat{H} = \hat{T} + \hat{V}$

Evaluate the expectation value $\langle \Phi | \hat{H} | \Phi \rangle = E[\rho]$ in a Slater determinant

→ Skyrme, Gogny, relativistic mean field (RMF) model

✓ Treat the **density $\boldsymbol{\rho(r)}$** as the fundamental variable and construct the energy density functional directly

→ Fayans energy density functional

Constraining Nuclear EDFs: Methods and Challenges

☐ How do we constrain nuclear EDFs?

Phenomenological coupling parameters

⟷

Bayesian inference

χ^2 minimization

Nuclear observables or Ab initio predictions

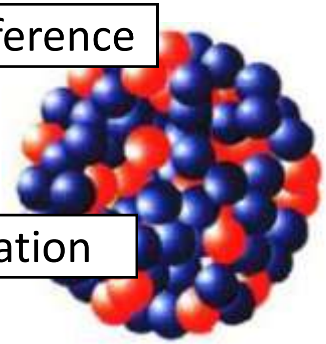

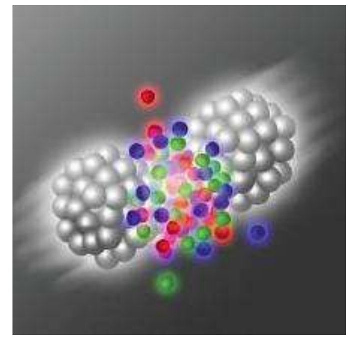

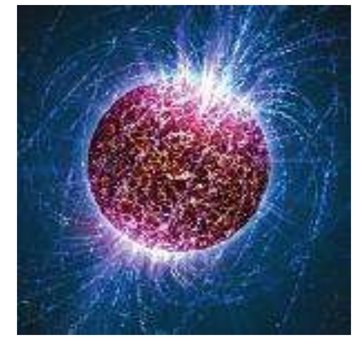

☐ What are the current difficulties faced by nuclear EDFs?

- ↪ Current experimental data are too limited / not precise enough to constrain the **isovector part of the nuclear EDFs.**
- ↪ Tensions between different constraints emerge and **cannot be simultaneously accommodated** by parameter tuning alone.

Example: Parity violating asymmetry

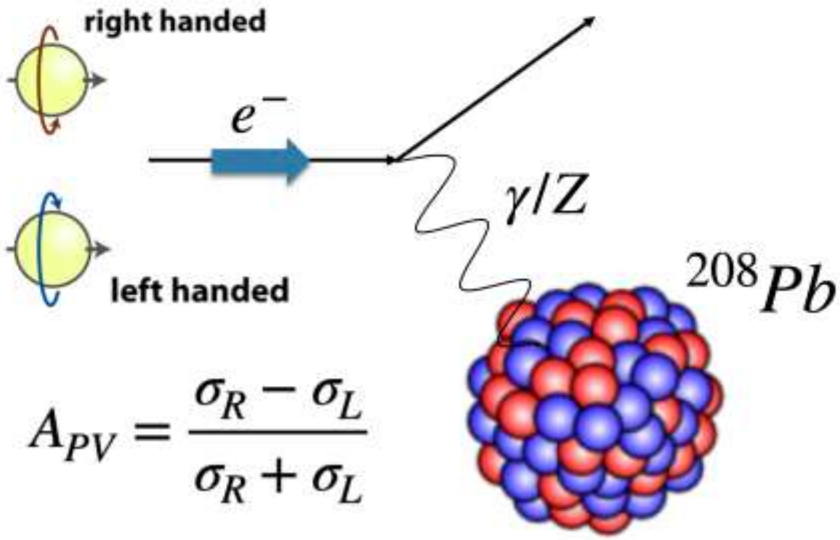

$$A_{PV} = \frac{\sigma_R - \sigma_L}{\sigma_R + \sigma_L}$$

Adhikari et al. (PREX), PRL126, 172502 (2021)

Reinhard, Roca-Maza, Nazarewicz, PRL 129, 232501 (2022)

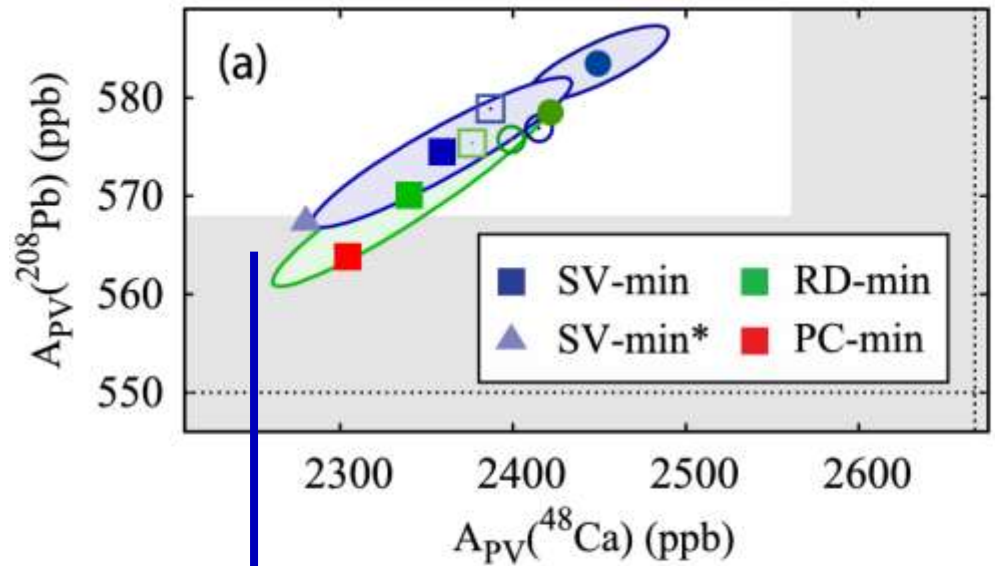

EDFs well calibrated to masses, radii, and surface thickness (and parity violating asymmetry, dipole polarizability)

- Sensitive to the isovector channel of the EDFs
- PREX2: Lead (^{208}Pb) Radius Experiment
- CREX: Calcium (^{48}Ca) Radius Experiment

No simultaneous description
Tensions exist for current EDFs !

Skyrme EDFs: Spin-orbit (SO) density

- Spin-orbit density (spherical nuclei)

$$J_q(r) = \frac{1}{4\pi r^3} \sum_i v_i^2 (2j_i + 1) \times \left[j_i(j_i+1) - l_i(l_i+1) - \frac{3}{4} \right] R_i^2(r)$$

- Contributions from $j_>$ and $j_<$ largely cancel with each other
  - $j_> = l + 1/2$: positive contribution
  - $j_< = l - 1/2$: negative contribution

- Spin orbit density is large in ^{48}Ca, but relatively small in ^{208}Pb
  - $^{48}\mathrm{Ca}$: $J_p \approx 0,\ J_n \gg 0$ (8 $1\mathrm{f}_{7/2}$ SO unpaired neutrons)
  - $^{208}\mathrm{Pb}$: $J_p \approx J_n \gg 0$ (14 $1\mathrm{i}_{13/2}$ neutron and 12 $1\mathrm{h}_{11/2}$ protons)

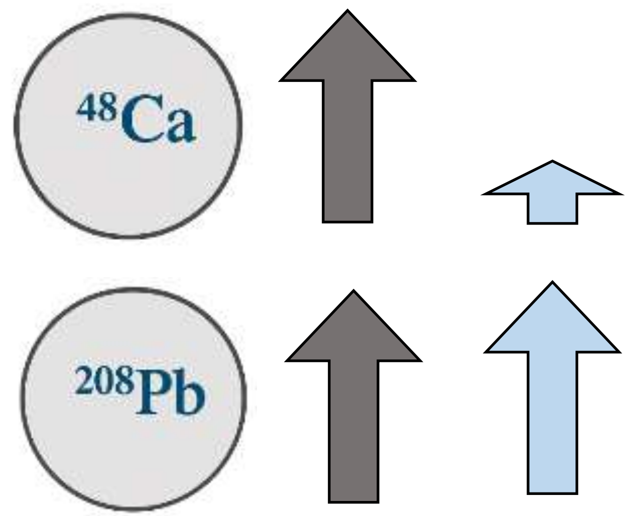

The isovector spin-orbit (IVSO) coupling is expected to have significant effects on ^{48}Ca while essentially no influence on ^{208}Pb!

Skyrme EDFs: CREX and PREX2

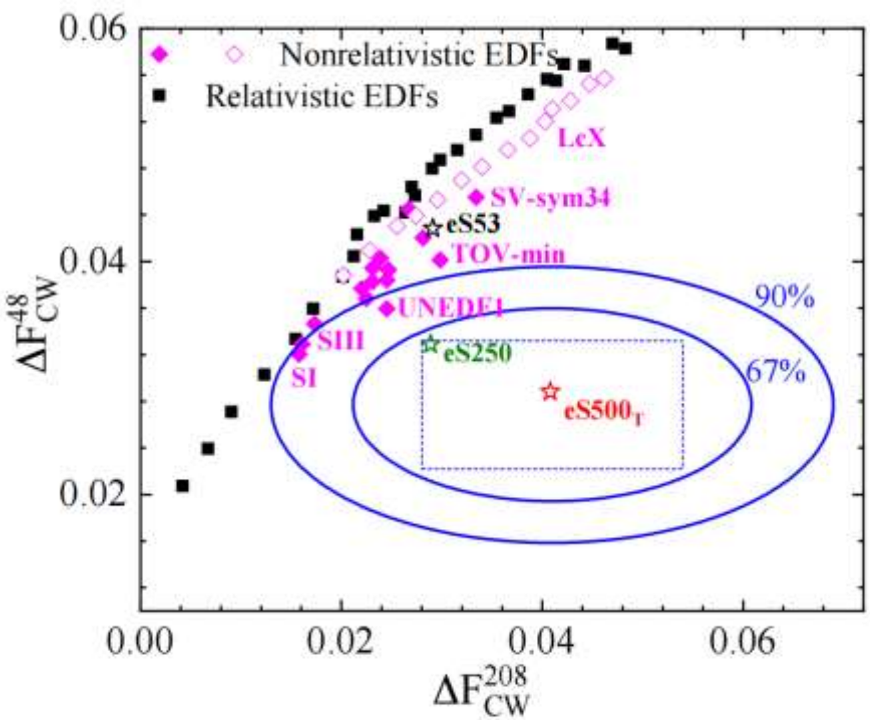

quantity	eS250	eS53	eS500$_T$	exp
r_c^{48} (fm)	3.4786	3.4642	3.5015	3.4771[64]
ΔF_{CW}^{48}	0.0329	0.0428	0.0288	0.0277 ± 0.0055[18]
Δr_{np}^{48} (fm)	0.130	0.181	0.105	
α_D^{48} (fm^3)	2.25	2.32	2.85	2.07 ± 0.22[37]
E_{GMR}^{208} (MeV)	13.78	13.78	13.55	

quantity	eS250	eS53	eS500$_T$	exp
r_c^{208} (fm)	5.4786	5.4793	5.5107	5.5012[64]
ΔF_{CW}^{208}	0.029	0.029	0.041	0.041 ± 0.013[19]
Δr_{np}^{208} (fm)	0.195	0.198	0.273	
α_D^{208} (fm^3)	20.12	19.84	22.98	19.60 ± 0.60[35,36]

T.G. Yue, Z. Zhang, L.W. Chen, arXiv: 2406.03844

😊The isovector spin-orbit coupling $b_{IV} \approx$ 500 MeV·fm^5 gives perfect fit to CREX/PREX2 data

😒The electric dipole polarizabilities are not compatible with experimental measurements when $b_{IV} \approx$ 500 MeV·fm^5

The isovector spin-orbit coupling b_{IV} should be larger than ≈ 250 MeV·fm^5 to fit CREX and PREX2 data

RMF: CREX and PREX2

$$\mathcal{L} = \bar{\psi}(i\gamma_\mu\partial^\mu - m)\psi - e\frac{1-\tau_3}{2}\bar{\psi}\gamma_\mu\psi A^\mu - \frac{1}{4}F_{\mu\nu}F^{\mu\nu}$$
$$-\frac{1}{2}\alpha_S(\bar{\psi}\psi)(\bar{\psi}\psi) - \frac{1}{2}\alpha_{\tau S}(\bar{\psi}\vec{\tau}\psi)(\bar{\psi}\vec{\tau}\psi)$$
$$-\frac{1}{2}\alpha_V\left(\bar{\psi}\gamma_\mu\psi\right)\left(\bar{\psi}\gamma^\mu\psi\right) - \frac{1}{2}\alpha_{\tau V}\left(\bar{\psi}\gamma_\mu\vec{\tau}\psi\right)\left(\bar{\psi}\gamma^\mu\vec{\tau}\psi\right)$$
$$-\frac{1}{2}\alpha_T\left(\bar{\psi}\sigma_{\mu\nu}\psi\right)\left(\bar{\psi}\sigma^{\mu\nu}\psi\right) - \frac{1}{2}\alpha_{\tau T}\left(\bar{\psi}\sigma_{\mu\nu}\vec{\tau}\psi\right)\left(\bar{\psi}\sigma^{\mu\nu}\vec{\tau}\psi\right)$$
$$-\frac{1}{2}\delta_S\partial_\mu(\bar{\psi}\psi)\partial^\mu(\bar{\psi}\psi)$$

Q. Zhao, et al. PRC 106, 034315 (2022)

isovector-scalar coupling

isoscalar tensor coupling

isovector tensor coupling

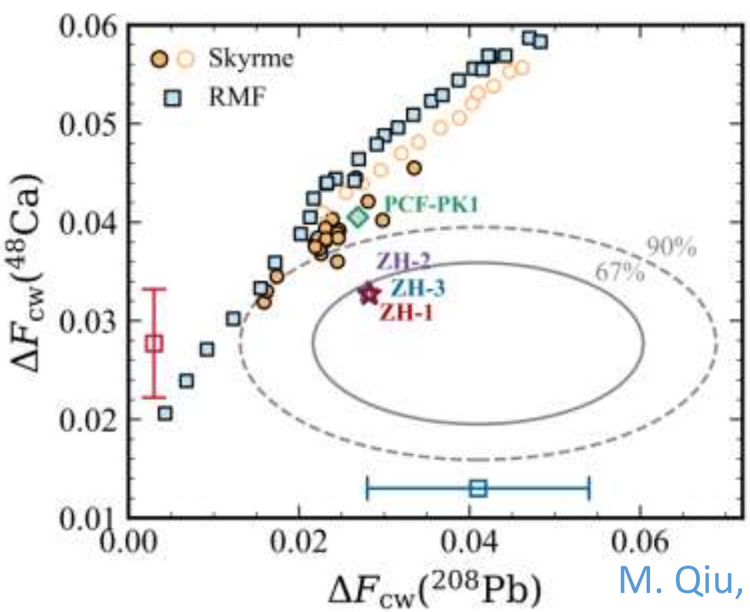

😊Charge-weak form factor differences in ^{48}Ca and ^{208}Pb: Consistent with PREX-II and CREX (67% C.L.)

😊Reasonable descriptions for binding energies, charge radius, spin-orbit splitting, single-particle energy levels and neutron matter equation of states

M. Qiu, Z. Zhang, T.G. Yue, L.W. Chen, arxiv: 2511.15385

RMF: Role of isovector spin-orbit (IVSO)

- By performing a nonrelativistic reduction, we found

$$b_{\rm IS} = 8\mathcal{B}_0^2\alpha_{\rm T} - 4\mathcal{B}_0^2\alpha_{\rm S} - 4\mathcal{B}_0^2\alpha'_{\rm S}\rho \qquad b_{\rm IV} = 8\mathcal{B}_0^2\alpha_{\tau\rm T} - 4\mathcal{B}_0^2\alpha_{\tau\rm S}$$

M. Qiu, Z. Zhang, T.G. Yue, L.W. Chen, arXiv: 2511.15385

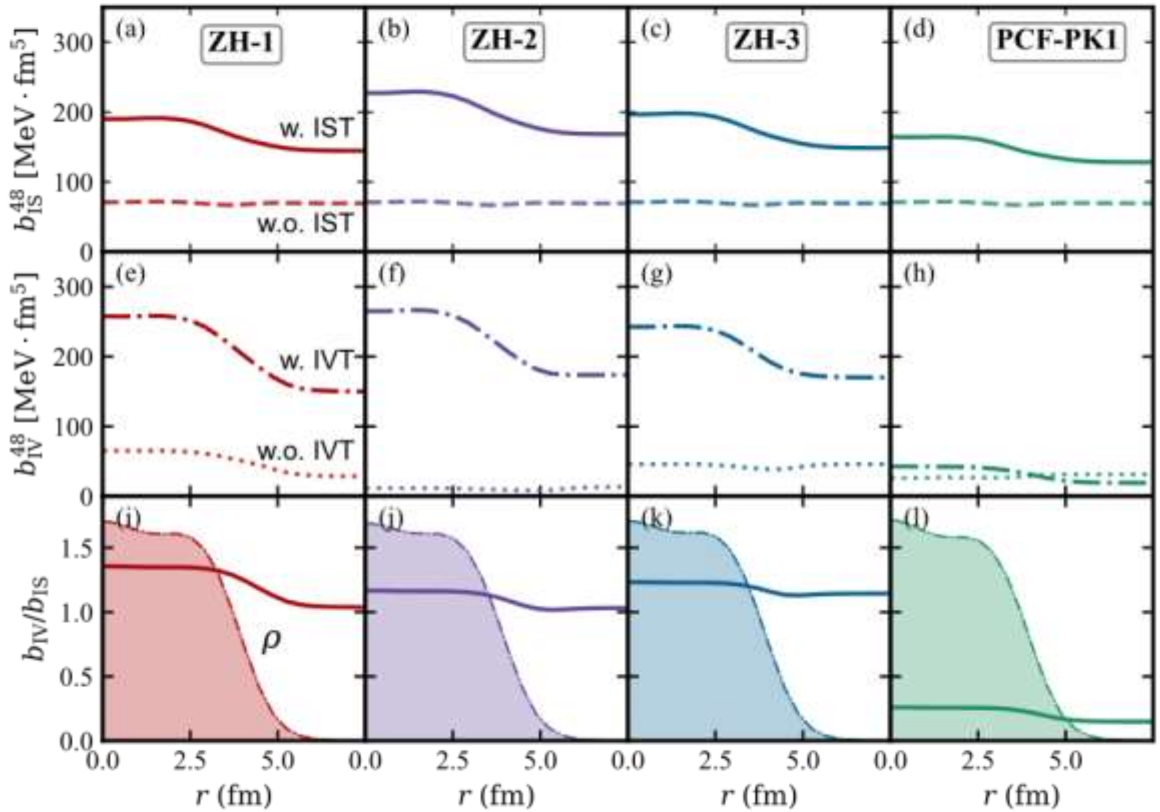

Similar ISSO coupling strength

Strong isovector tensor coupling leads to strong IVSO coupling strengths

IVSO in new series > PCF-PK1

Confirms again the possible role of IVSO coupling

Future plan: Fayans nuclear EDFs

- Starting directly from the energy density functional, Fayans EDF is constructed by

$$\mathcal{E} = \mathcal{E}_{\text{kin}} + \mathcal{E}_{\text{nuc}} + \mathcal{E}_{\text{Coul}} + \mathcal{E}_{\text{ls}} + \mathcal{E}_{\text{pairing}}$$

S. A. Fayans, JETP Lett., Vol. 68, No. 3, 10 August 1998

- Volumne and surface term

More sophisticated density dependence

$$\mathcal{E}_v = \frac{2}{3}\varepsilon_F^0 \rho_0 [a_\alpha^v f_\alpha(\alpha,\beta,\nabla\alpha,...)\alpha^2 + a_\beta^v f_\beta(\alpha,\beta,\nabla\alpha,...)\beta^2]$$

$$\mathcal{E}_s = \frac{2}{3}\varepsilon_F^0 \rho_0 r_0^2 [a_\alpha^v g_\alpha(\alpha,\beta,\nabla\alpha,...)(\nabla\alpha)^2 + a_\beta^s g_\beta(\alpha,\beta,\nabla\alpha,...)(\nabla\beta)^2]$$

$$f_t(\alpha) = \frac{1 - b_t^v \alpha^{\sigma_t^v}}{1 + c_t^v \alpha^{\sigma_t^v}}, \qquad t = \alpha, \beta.$$

$$g_t(\alpha, \beta, \nabla\alpha, \ldots) = \frac{1}{1 + c_t^s \alpha^{\sigma_t^s} + d_t^s r_0^2 (\nabla\alpha)^2}$$

- Pairing term

More flexibility in pairing

$$\mathcal{E}_{\text{pairing}} = \sum_{q=n,p} \frac{2}{3} \frac{\varepsilon_F^0}{\rho_0} a_q^{\text{pair}} \kappa_q^\dagger f_{\text{pair}}(\alpha,\beta,\nabla\alpha,...)\kappa_q$$

$$f_{\text{pair}}(\alpha, \beta, \nabla\alpha, \ldots) = 1 - b_{\text{pair}}\, \alpha^{\sigma_{\text{pair}}} + d_{\text{pair}}\, r_0^2 (\nabla\alpha)^2$$

Fayans EDFs show advantages in charge radii systematics

Conclusion: The Fayans paring functional, with its generalized density dependence, significantly improves the description of charge radii in odd and even nuclei. Adding differential charge radii to the set of fit observables

P.-G. Reinhard and W. Nazarewicz, PRC 95, 064328 (2017)

Towards Improved EDFs via Bayesian Inference

Question 1: Can current Fayans EDFs simultaneously accommodate the PREX2 and CREX data without compromising other ground state properties?

Bayesian parameter estimations

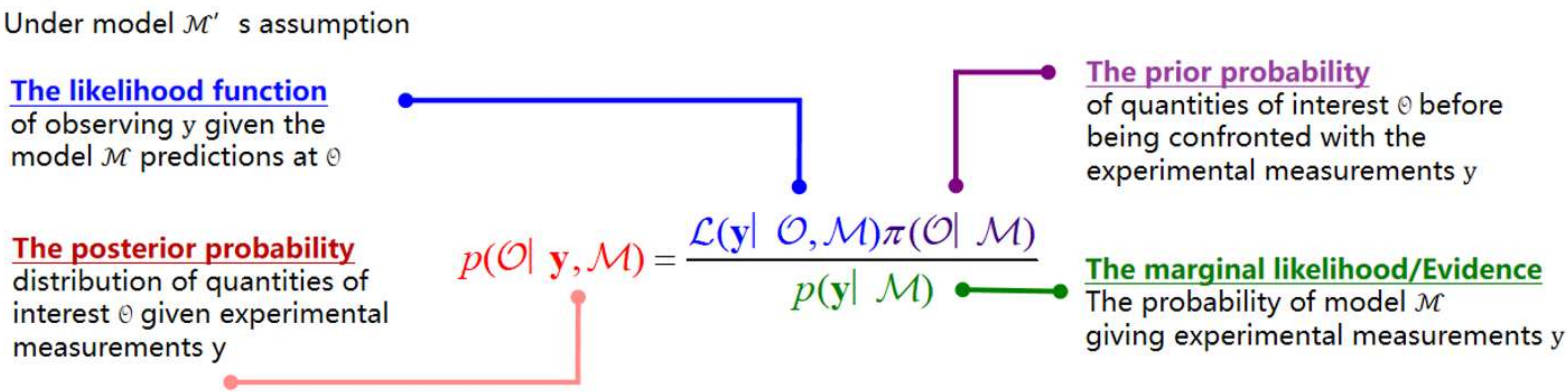

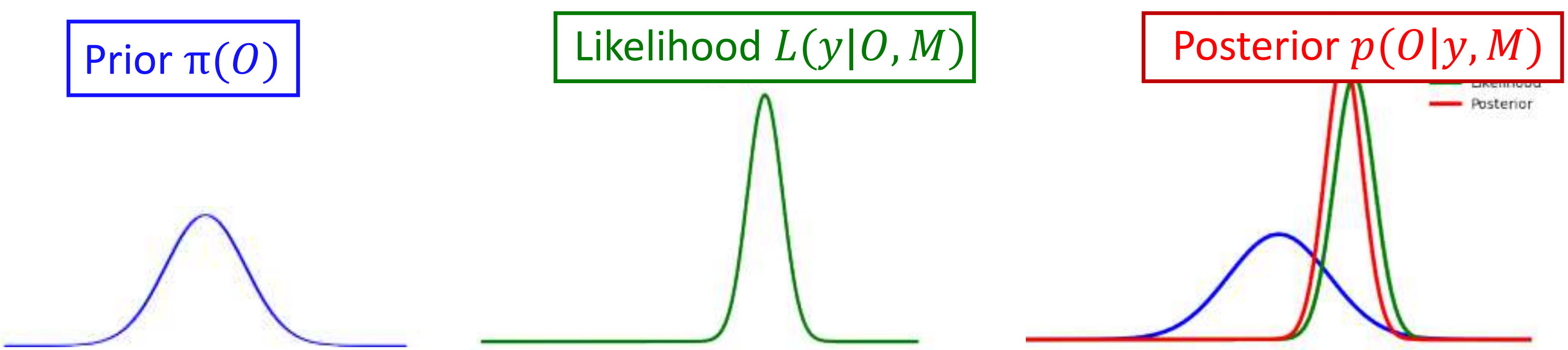

Towards Improved EDFs via Bayesian Inference

Question 1: Can current Fayans EDFs simultaneously accommodate the PREX2 and CREX data without compromising other ground state properties?

Bayesian parameter estimations

Question 2: **If not**, which aspects of the Fayans functional form should be generalized or extended?

- ✓ Additional isovector spin-orbit coupling term?
- ✓ Additional isovector surface term?
- ✓ Different density dependence?

Guided by Bayesian model comparisons

→ An increase in the number of the phenomenological parameters

✦ **Evidence** (a larger evidence indicates a better model)

$$Z \equiv p(\boldsymbol{y} \mid M) = \int d\boldsymbol{\theta} L(\boldsymbol{y} \mid M, \theta) \pi(\boldsymbol{\theta} \mid M)$$

$$\approx L\left(\boldsymbol{y} \mid M, \theta_{\mathrm{ML}}\right) \left(\Delta\theta_{\mathrm{like}} / \Delta\theta_{\mathrm{prior}}\right)^{N_\theta}$$

Maximum likelihood

No. of parameter, model complexity

Udo von Toussaint, Rev. Mod. Phys. 83, 943 (2011)

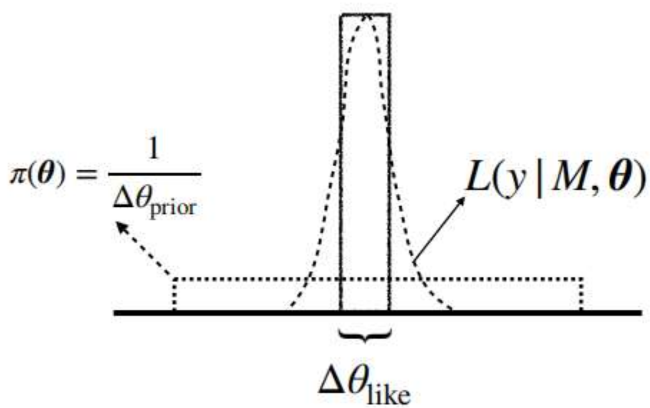

Conclusion and Outlook

- Current nuclear energy density functionals are unable to simultaneously describe the PREX2 and CREX data, indicating **the need for further improvements.**

- Existing analyses from Skyrme and relativistic mean field (RMF) frameworks: **a larger isovector spin-orbit (IVSO) coupling strength** than previously assumed may play a key role in reconciling the two measurements.

- **Future work**: Bayesian-guided **extensions of Fayans energy density functionals** for improved descriptions of finite nuclei, including PREX-II, CREX, and other ground-state properties

Thank you!

ZH series: Parameters

	PCF-PK1	ZH-1	ZH-2	ZH-3
$\alpha_{\tau S}(\rho_{sat})$	-1.981	-4.701	-0.8403	-3.321
$a_{\tau S}$	2.328	0.5947	2.126	1.802
$b_{\tau S}$	0.06179	84.914	334.1	9.290
$c_{\tau S}$	0.5704	50.16	711.5	17.36
$d_{\tau S}$	0.7644	0.08152	0.02165	0.1386
$\alpha_{\tau V}(\rho_{sat})$	2.976	5.400	1.927	4.096
$a_{\tau V}$	2.547	4.212	9.430	6.656
$b_{\tau V}$	0.3459	-0.001241	-0.001728	-0.002950
$c_{\tau V}$	1.612	0.0006678	0.0007385	0.001406
$d_{\tau V}$	0.4547	22.34	21.24	15.39
δ_S	-0.6658	-0.7173	-0.7886	-0.7311
α_T	3.374	4.312	5.673	4.546
$\alpha_{\tau T}$	0.535[a]	6.967	9.195	7.114
ΔF_{CW}^{48}	0.0405	0.0327	0.0329	0.0326
ΔF_{CW}^{208}	0.0269	0.0284	0.0280	0.0282
Δr_{np}^{48}	0.172	0.116	0.128	0.127
Δr_{np}^{208}	0.183	0.188	0.190	0.191
$E_{sym}(\rho_{sat})$	33.0	33.6	32.4	32.1
$E_{sym}(2\rho_{sat}/3)$	24.5	25.4	25.8	26.9
L	78.4	66.7	43.8	19.4
$L(2\rho_{sat}/3)$	50.4	54.2	50.2	49.0
K_{sym}	61.4	-114	-276	-469
$\langle b_{IS}^{(48)}\rangle$	150	172	205	178
$\langle b_{IS}^{(208)}\rangle$	153	176	210	182
$\langle b_{IV}^{(48)}\rangle$	35.0	222	230	213
$\langle b_{IV}^{(208)}\rangle$	36.7	229	238	219

[a] The maximum value of $\alpha_{\tau T}$ in ^{48}Ca in PCF-PK1.

Density dependent point-coupling RMF

$$\mathcal{L}=\bar{\psi}(i\gamma_\mu\partial^\mu-m)\psi-e\frac{1-\tau_3}{2}\bar{\psi}\gamma_\mu\psi A^\mu-\frac{1}{4}F_{\mu\nu}F^{\mu\nu}$$

Q. Zhao, et al. PRC 106, 034315 (2022)

$$-\frac{1}{2}\alpha_S(\bar{\psi}\psi)(\bar{\psi}\psi)-\frac{1}{2}\alpha_{\tau S}(\bar{\psi}\vec{\tau}\psi)(\bar{\psi}\vec{\tau}\psi)$$

isovector-scalar coupling

$$-\frac{1}{2}\alpha_V\left(\bar{\psi}\gamma_\mu\psi\right)\left(\bar{\psi}\gamma^\mu\psi\right)-\frac{1}{2}\alpha_{\tau V}\left(\bar{\psi}\gamma_\mu\vec{\tau}\psi\right)\left(\bar{\psi}\gamma^\mu\vec{\tau}\psi\right)$$

$$-\frac{1}{2}\alpha_T\left(\bar{\psi}\sigma_{\mu\nu}\psi\right)\left(\bar{\psi}\sigma^{\mu\nu}\psi\right)-\frac{1}{2}\alpha_{\tau T}\left(\bar{\psi}\sigma_{\mu\nu}\vec{\tau}\psi\right)\left(\bar{\psi}\sigma^{\mu\nu}\vec{\tau}\psi\right)$$

isoscalar tensor coupling
isovector tensor coupling

$$-\frac{1}{2}\delta_S\partial_\mu(\bar{\psi}\psi)\partial^\mu(\bar{\psi}\psi)$$

- Density dependent ansatz for S, V, τS, τV

$$\alpha_i(\rho)=\alpha_i(\rho_{sat})f_i(x),\quad f_i(x)=a_i\frac{1+b_i(x+d_i)^2}{1+c_i(x+d_i)^2}$$

$$f_i(1)=1,f_i''(0)=0$$

- In PCF-PK1, $\alpha_{\tau T}$ determined from Fierz transformation

$$\alpha_{tT}=\frac{1}{18}(-\alpha_S+3\alpha_{\tau S}+2\alpha_V-6\alpha_{\tau V}+6\alpha_T)$$

- **We treat ατT as a free density-independent parameter**
- Keeping the isoscalar channels unchanged, the remaining parameters are calibrated to:
  - Form factor difference of ^{48}Ca and ^{208}Pb
  - Ground states properties of ^{48}Ca and ^{208}Pb
  - Properties of nuclear matter equation of states

Three new relativistic EDFs : ZH-1,2,3

- Charge density and weak density in ^{48}Ca and ^{208}Pb

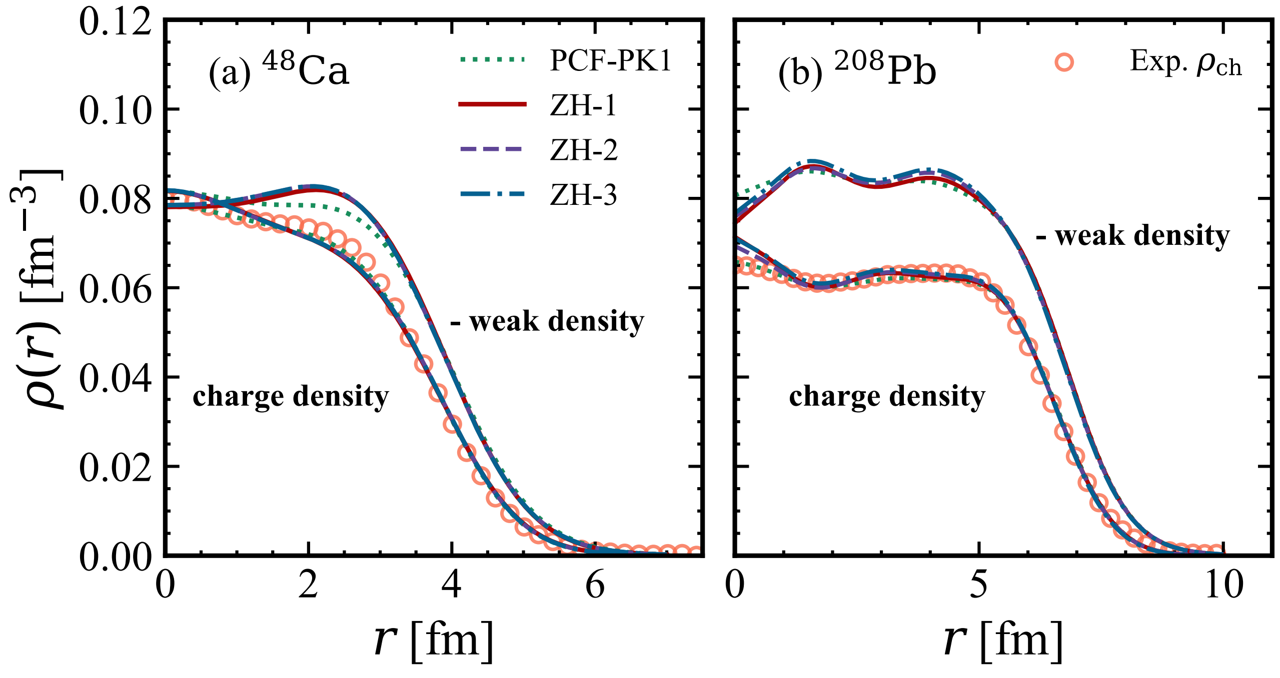

M. Qiu, Z. Zhang, T.G. Yue, L.W. Chen, in preparation

No unphysical density fluctuations in the nuclear interior

Three new relativistic EDFs : ZH-1,2,3

- Binding energies and charge radius

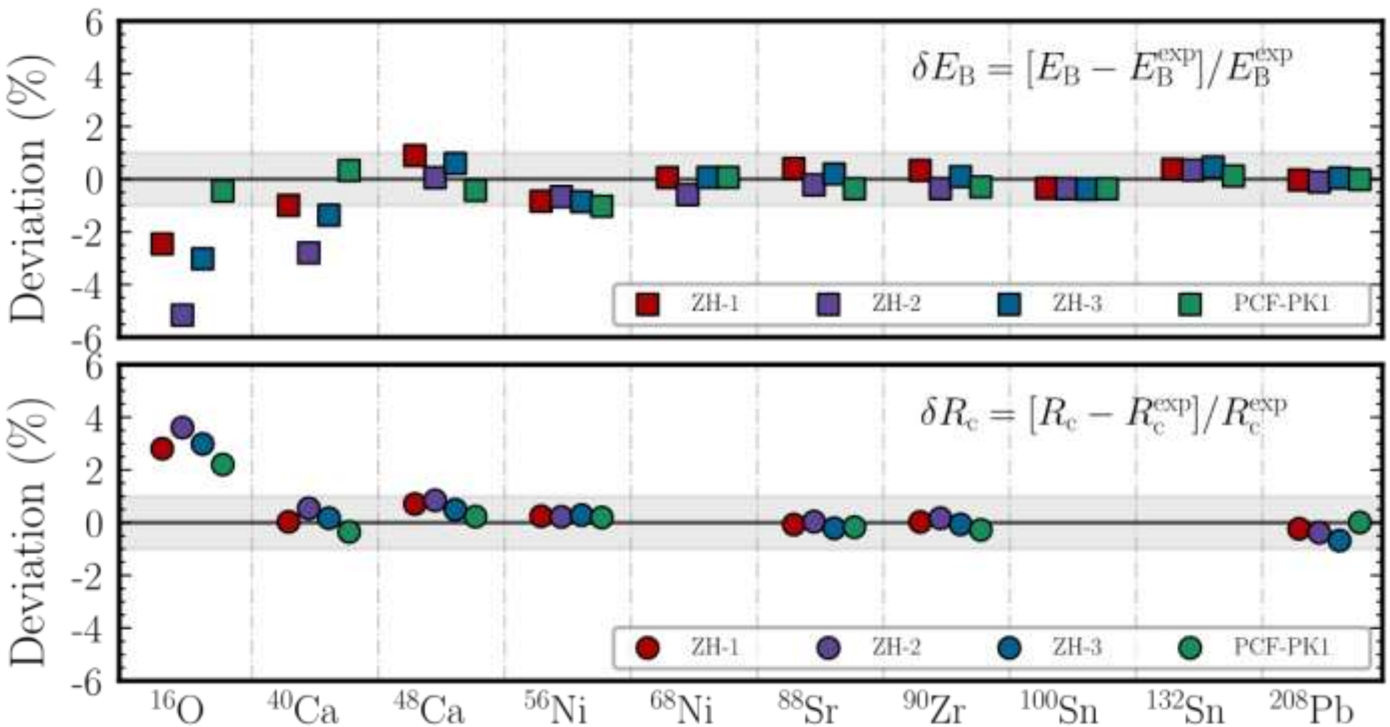

M. Qiu, Z. Zhang, T.G. Yue, L.W. Chen, in preparation

Reasonable description for ground state properties of (semi-) doubly magic nuclei

Three new relativistic EDFs : ZH-1,2,3

- Pure neutron matter equation of state

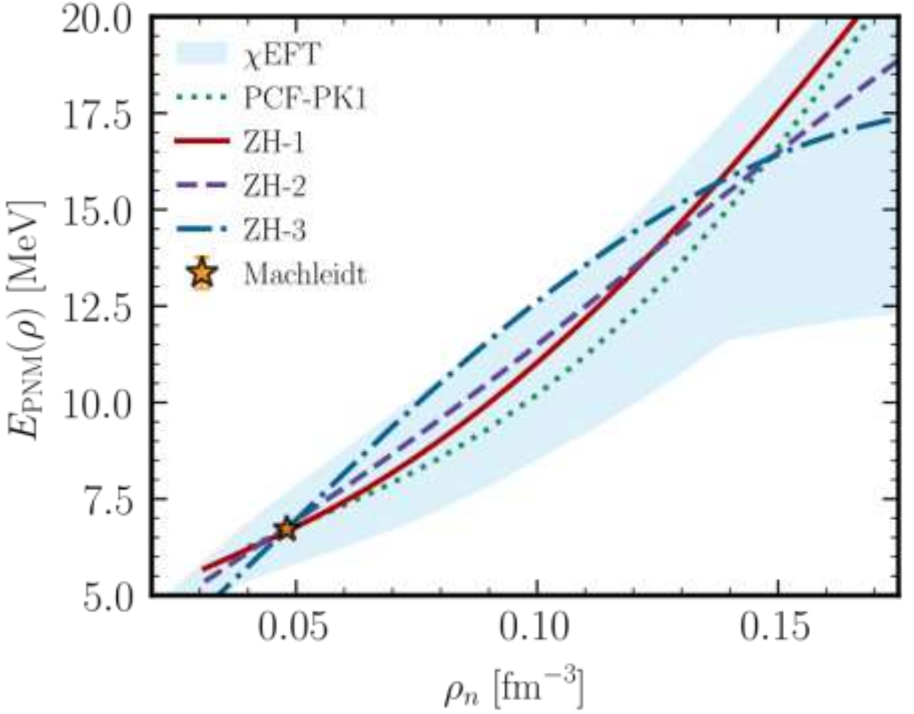

M. Qiu, Z. Zhang, T.G. Yue, L.W. Chen, in preparation

Reasonable description for neutron matter equation of state

ZH series: SO splittings

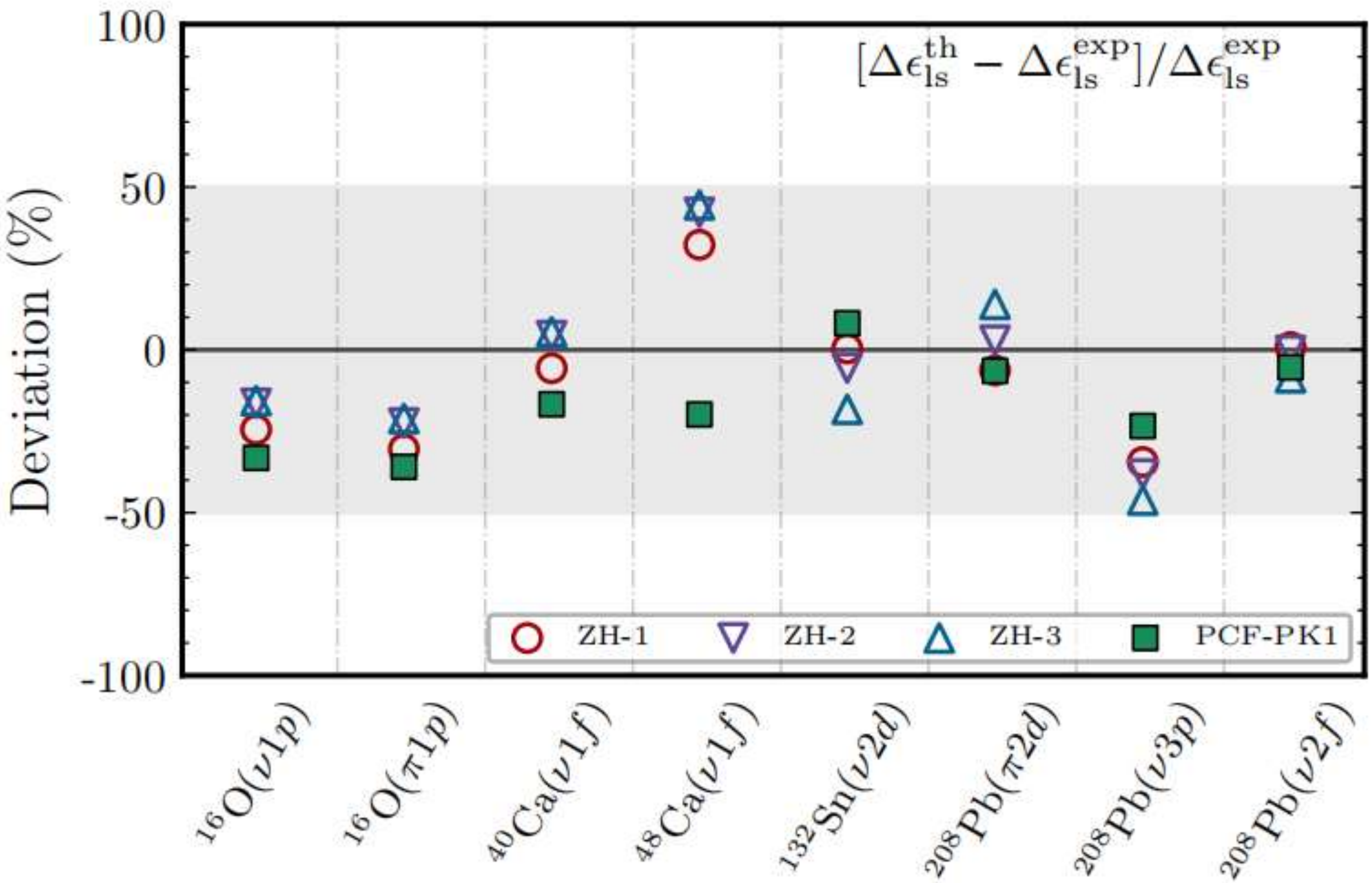

Non-relativistic reduction

Density-dependent point-coupling potential energy density

$$\mathcal{E} = \frac{1}{2}\alpha_S\rho_S^2 + \frac{1}{2}\alpha_V\rho_V^2 + \frac{1}{2}\alpha_{\tau S}\rho_{\tau S}^2 + \frac{1}{2}\alpha_{\tau V}\rho_{\tau V}^2 - \alpha_{\tau T}\, j_{\tau T}^{0\,2} - \alpha_T\, j_T^{0\,2} - \frac{1}{2}\delta_S(\nabla\rho_S)^2$$

$\boldsymbol{\rho_S}$, $\boldsymbol{\rho_V}$, $\mathbf{j_T^0}$ In expression of ρ, τ, $\boldsymbol{J}$

Non-relativistic Skyrme energy density

$$\mathcal{E} = b_0\rho^2 + b_3\rho^{2+\alpha} + b_2\rho\Delta\rho + b_1\rho\tau + \frac{b_{IS}}{2}\rho\nabla J \quad \text{Isoscalar}$$

$$\tilde{b}_0\tilde{\rho}^2 + \tilde{b}_3\tilde{\rho}^2\rho^\alpha + \tilde{b}_2\tilde{\rho}\Delta\tilde{\rho} + \tilde{b}_1\tilde{\rho}\tilde{\tau} + \frac{b_{IV}}{2}\tilde{\rho}\nabla\tilde{J} \quad \text{Isovector}$$

density dependent | gradient | Kinetic | Spin-orbit

Non-relativistic reduction

- Dirac equation

$$\begin{pmatrix} m+S+V^0 & \boldsymbol{\sigma}\cdot(\boldsymbol{p}-i\boldsymbol{T}^0) \\ \boldsymbol{\sigma}\cdot(\boldsymbol{p}+i\boldsymbol{T}^0) & -m-S+V^0 \end{pmatrix}\begin{pmatrix}\varphi\\ \chi\end{pmatrix}=\epsilon\begin{pmatrix}\varphi\\ \chi\end{pmatrix}$$

- Eliminating the lower component of the Dirac spinor

$$\chi=\frac{\boldsymbol{\sigma}\cdot(\boldsymbol{p}+i\boldsymbol{T}^0)}{\epsilon+m+S-V^0}\varphi\equiv\mathcal{B}\boldsymbol{\sigma}\cdot\vec{\Pi}\varphi \qquad \mathcal{B}=[\epsilon+m+S-V^0]^{-1} \qquad \vec{\Pi}=\boldsymbol{p}+i\boldsymbol{T}^0$$

- Normalization condition

$$\int d^3r\bar{\psi}\gamma^0\psi=\int \mathrm{d}^3r\varphi^\dagger\hat{I}\varphi=1=\int \mathrm{d}^3r\phi^{\mathrm{cl}\dagger}\phi^{\mathrm{cl}} \qquad \hat{I}=1+\boldsymbol{\sigma}\cdot\overleftarrow{\Pi}\mathcal{B}^2\boldsymbol{\sigma}\cdot\overrightarrow{\Pi}$$

$$\varphi=\hat{I}^{-1/2}\phi^{\mathrm{cl}}$$

- Order counting

$$S+V^0\sim v^2,$$

$$\epsilon-m\sim v^2,$$

$$\boldsymbol{\sigma}\cdot(\boldsymbol{p}-i\boldsymbol{T}^0)\mathcal{B}\boldsymbol{\sigma}\cdot\vec{\Pi}\sim v^2$$

Non-relativistic reduction

- Non-relativistic limit of relevant current and density

$$
\begin{aligned}
\rho_{\mathrm{V}} &= \rho, \\
\rho_{\mathrm{S}} &= \sum \phi^{\mathrm{cl}\dagger} \hat{I}^{-1/2} \left(1 - \boldsymbol{\sigma} \cdot \overleftarrow{\Pi} \mathcal{B}_0^2 \boldsymbol{\sigma} \cdot \overrightarrow{\Pi}\right) \hat{I}^{-1/2} \phi^{\mathrm{cl}} \\
&= \rho - 2\mathcal{B}_0^2 \left[\tau - \nabla \boldsymbol{J} - \nabla\rho \cdot \boldsymbol{T}^0 + 2\boldsymbol{T}^0 \cdot \boldsymbol{J} + \rho {\boldsymbol{T}^0}^2\right], \\
\mathbf{j}_{\mathrm{T}}^0 &= \sum \left[\phi^{\mathrm{cl}\dagger} \hat{I}^{-1/2} \left(i\boldsymbol{\sigma} \mathcal{B}_0 \boldsymbol{\sigma} \overrightarrow{\Pi}\right) \hat{I}^{-1/2} \phi^{\mathrm{cl}} - c.c\right] \\
&= \mathcal{B}_0 \nabla\rho - 2\mathcal{B}_0 \boldsymbol{T}^0 \rho - 2\mathcal{B}_0 \boldsymbol{J}.
\end{aligned}
$$

- Non-relativistic limit of the potential energy density

$$
\begin{aligned}
\mathcal{E} = &\left(\frac{1}{2}\alpha_{\mathrm{S}} + \frac{1}{2}\alpha_{\mathrm{V}}\right)\rho^2 + \left(\frac{1}{2}\alpha_{\tau\mathrm{S}} + \frac{1}{2}\alpha_{\tau\mathrm{V}}\right)\tilde{\rho}^2 - \frac{1}{2}\delta_{\mathrm{S}}(\nabla\rho)^2 - 2\mathcal{B}_0^2\alpha_{\mathrm{S}}\rho\tau - 2\mathcal{B}_0^2\alpha_{\tau\mathrm{S}}\tilde{\rho}\tilde{\tau} \\
&- \alpha_{\mathrm{T}}\mathcal{B}_0^2(\nabla\rho)^2 - \alpha_{\tau\mathrm{T}}\mathcal{B}_0^2\left(\nabla\tilde{\rho}\right)^2 - 4\alpha_{\mathrm{T}}\mathcal{B}_0^2\boldsymbol{J}^2 - 4\alpha_{\tau\mathrm{T}}\mathcal{B}_0^2\tilde{\boldsymbol{J}}^2 - \boxed{2\mathcal{B}_0^2\alpha'_{\tau\mathrm{S}}\tilde{\rho}\nabla\rho} \cdot \tilde{\boldsymbol{J}} \\
&\boxed{+ \left(-2\mathcal{B}_0^2\alpha'_{\mathrm{S}}\rho - 2\mathcal{B}_0^2\alpha_{\mathrm{S}} + 4\mathcal{B}_0^2\alpha_{\mathrm{T}}\right)}\nabla\rho \cdot \boldsymbol{J} + \boxed{\left(-2\mathcal{B}_0^2\alpha_{\tau\mathrm{S}} + 4\mathcal{B}_0^2\alpha_{\tau\mathrm{T}}\right)}\nabla\tilde{\rho} \cdot \tilde{\boldsymbol{J}}
\end{aligned}
$$

- Non-relativistic limit of the SO coupling strength

$$
b_{\mathrm{IS}} = 8\mathcal{B}_0^2\alpha_{\mathrm{T}} - 4\mathcal{B}_0^2\alpha_{\mathrm{S}} - 4\mathcal{B}_0^2\alpha'_{\mathrm{S}}\rho \qquad b_{\mathrm{IV}} = 8\mathcal{B}_0^2\alpha_{\tau\mathrm{T}} - 4\mathcal{B}_0^2\alpha_{\tau\mathrm{S}} \qquad b_{\mathrm{SV}} = -4\mathcal{B}_0^2\alpha'_{\tau\mathrm{S}}\tilde{\rho}
$$

ISSO coupling | IVSO coupling | SVSO coupling

ZH series: SO partner ordering

- Single particles energies of ^{48}Ca

M. Qiu, Z. Zhang, T.G. Yue, L.W. Chen, in preparation

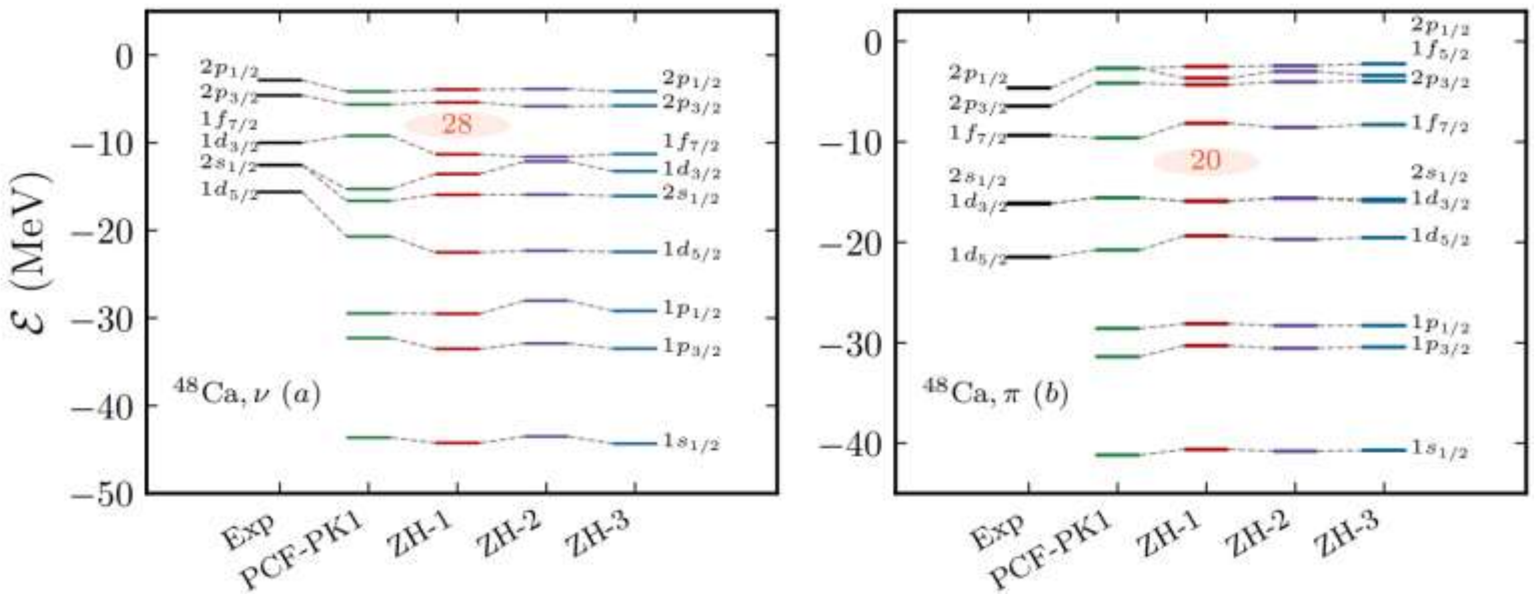

Different from meson-exchange RMF case
- ✓ Right ordering of SO partners
- ✓ Shell closures

What results in the difference?

Central average mean field v.s. SO potential

ZH-series

Starting from energy density in non-relativistic limit, we derive

Averaged central potential

$$U_q = (\alpha_{\mathrm{S}} + \alpha_{\mathrm{V}})\rho + \tau_3(\alpha_{\tau\mathrm{S}} + \alpha_{\tau\mathrm{V}})\tilde{\rho} + \frac{1}{2}(\alpha'_{\mathrm{S}} + \alpha'_{\mathrm{S}})\rho^2 + \frac{1}{2}(\alpha'_{\tau\mathrm{S}} + \alpha'_{\tau\mathrm{S}})\tilde{\rho}^2$$
$$- 2\mathcal{B}_0^2\alpha_{\mathrm{S}}\tau - 2\tau_3\mathcal{B}_0^2\alpha_{\tau\mathrm{S}}\tilde{\tau} - 2\mathcal{B}_0^2\alpha'_{\mathrm{S}}\rho\tau - 2\mathcal{B}_0^2\alpha'_{\tau\mathrm{S}}\tilde{\tau}$$
$$+ (2\mathcal{B}_0^2\alpha_{\mathrm{T}} + \delta_{\mathrm{S}})\nabla^2\rho + 2\tau_3\mathcal{B}_0^2\alpha_{\tau\mathrm{T}}\nabla^2\tilde{\rho}$$
$$- \frac{b_{\mathrm{IS}}}{2}\nabla\boldsymbol{J} + \tau_3\frac{b_{\mathrm{IV}} + \tau_3 b_{\mathrm{SV}}}{2}\nabla\tilde{\boldsymbol{J}}$$

Spin-orbit potential

$$U_{so} = \frac{b_{\mathrm{IS}} + \tau_3 b_{\mathrm{SV}}}{2}\nabla\rho + \tau_3\frac{b_{\mathrm{IV}}}{2}\nabla\tilde{\rho} + 8\mathcal{B}_0^2\alpha_{\mathrm{T}}\boldsymbol{J} - 8\tau_3\mathcal{B}_0^2\alpha_{\tau\mathrm{T}}\tilde{\boldsymbol{J}}$$

Kunjipurayil et al.

Only SO potential is modified

Spin-orbit potential $Uso \rightarrow U_{so}^{(0)}(r) \pm \beta U_{so}^{(1)}(r)$

A.Kunjipurayil, J. Piekarewicz, M. Salinas, Phys. Rev. C 112, 014310

All orbitals contributes to the changes

Main contributions from central potential

Relatively small enhancement is required

A crazy β is needed

Main contribution from SO potential

changes largely due to the unpaired $f_{7/2}$ neutrons

Central average mean field v.s. SO potential

In Skyrme-like EDFs

$$\hat{h}_q = -\nabla \cdot \frac{\hbar^2}{2m_q^*}\nabla + U_q + i\boldsymbol{W}_q \cdot (\boldsymbol{\sigma} \times \nabla),$$

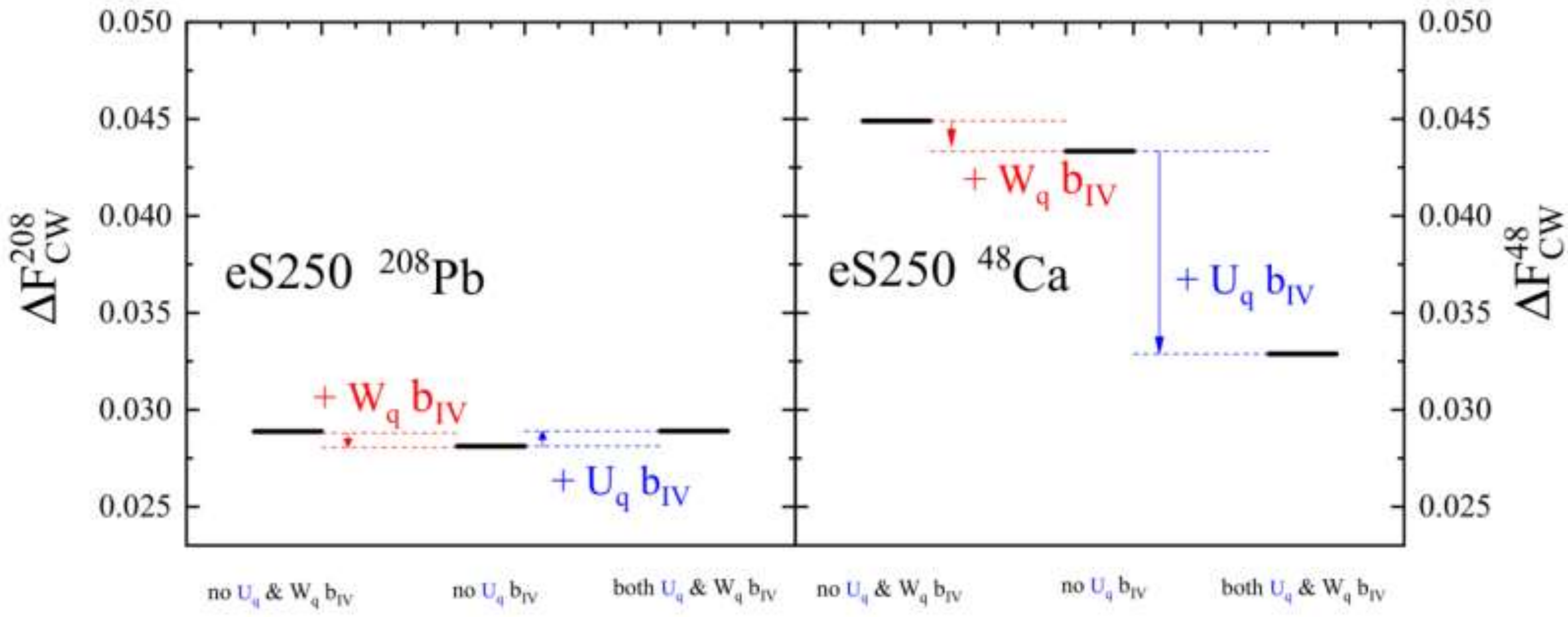

IVSO effects in U_q dominate ! ! !

Central average mean field v.s. SO potential

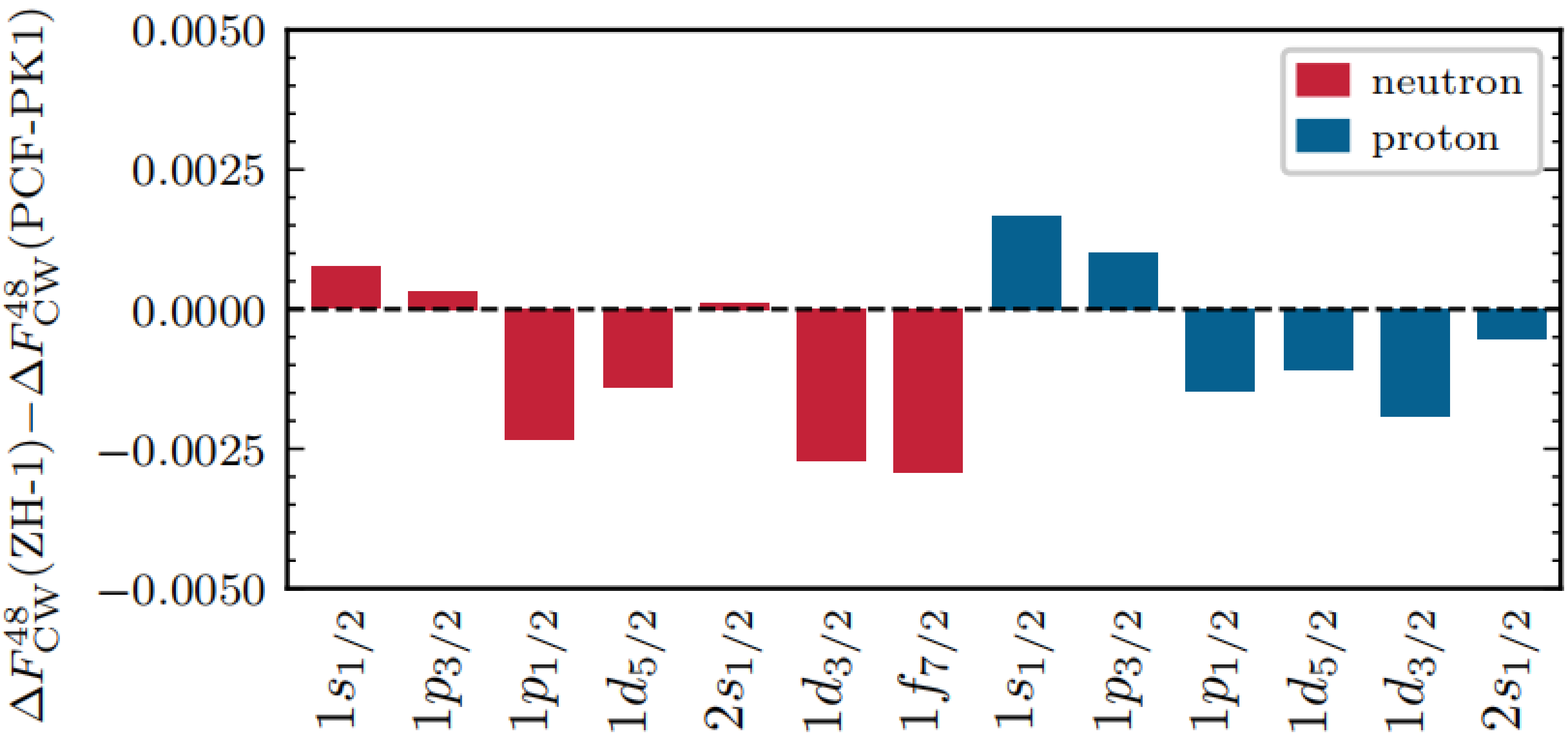

ZH series: correlations

M. Qiu, Z. Zhang, T.G. Yue, L.W. Chen, in preparation

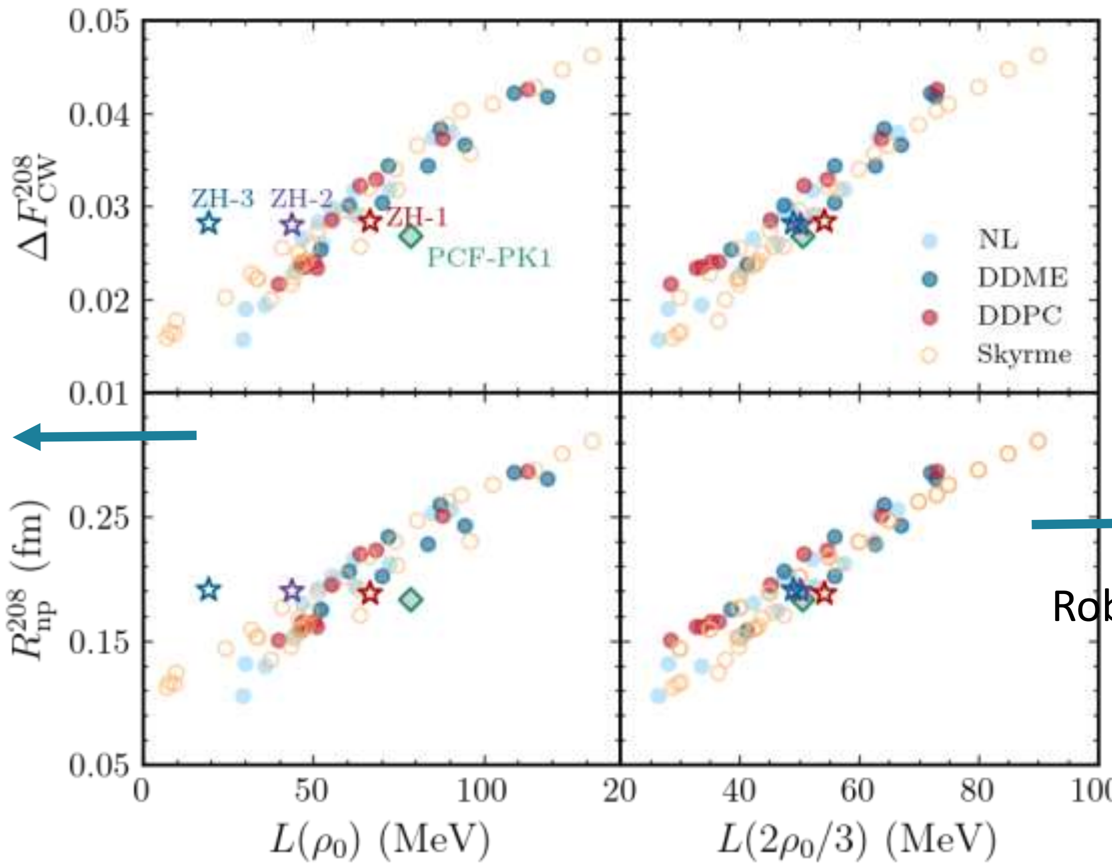

Weak $R_{np} - L$ correlation

Robust $R_{np} - L(2\rho_0/3)$

- Weak-charge form factor differences of ^{48}Ca as a probe of IVSO coupling strength
- Neutron skin of ^{208}Pb as a probe of $L(2\rho_0/3)$ instead of L

ZH series: correlation

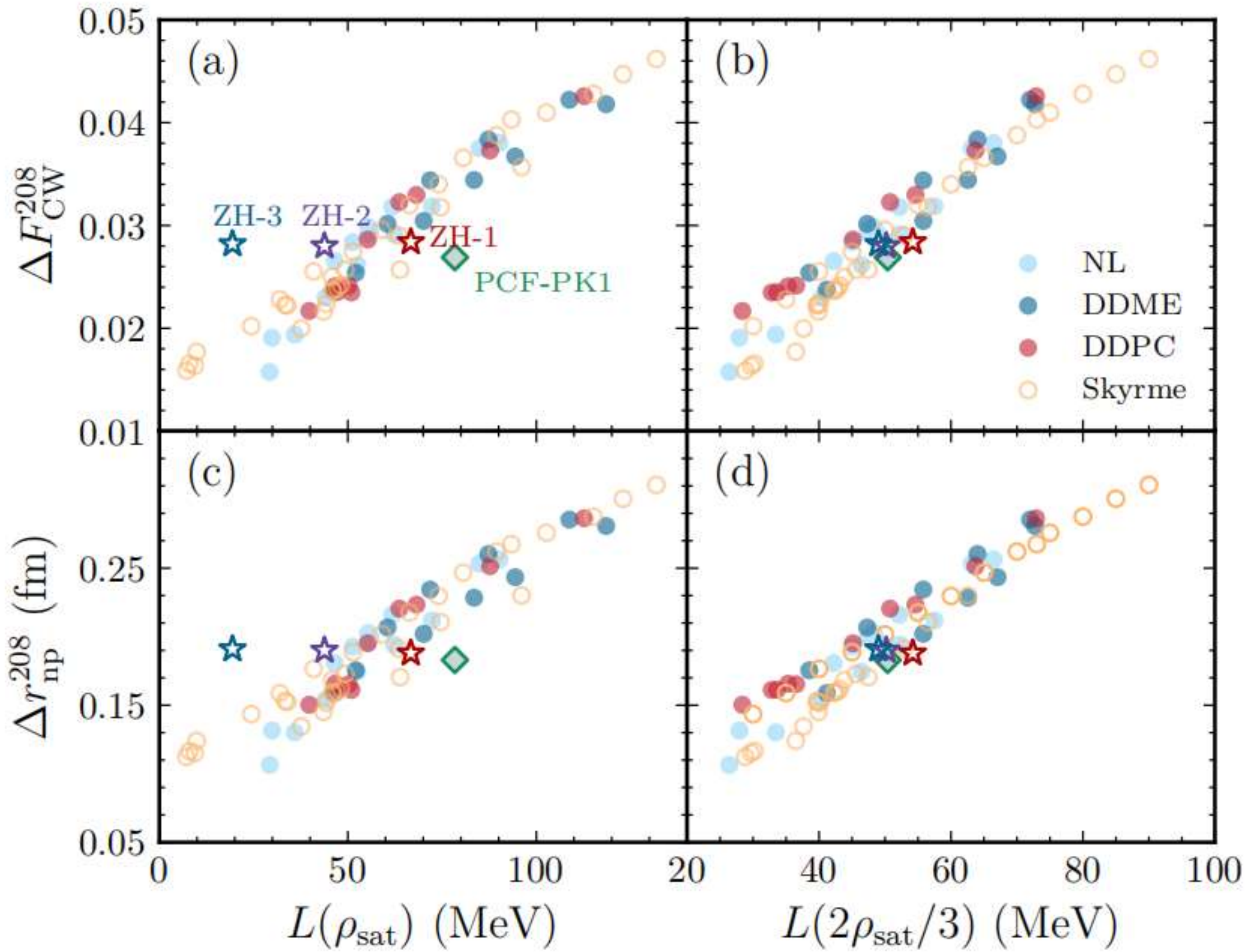

Spin-orbit interaction and neutron skin

Sensitivity analysis based on MSL0

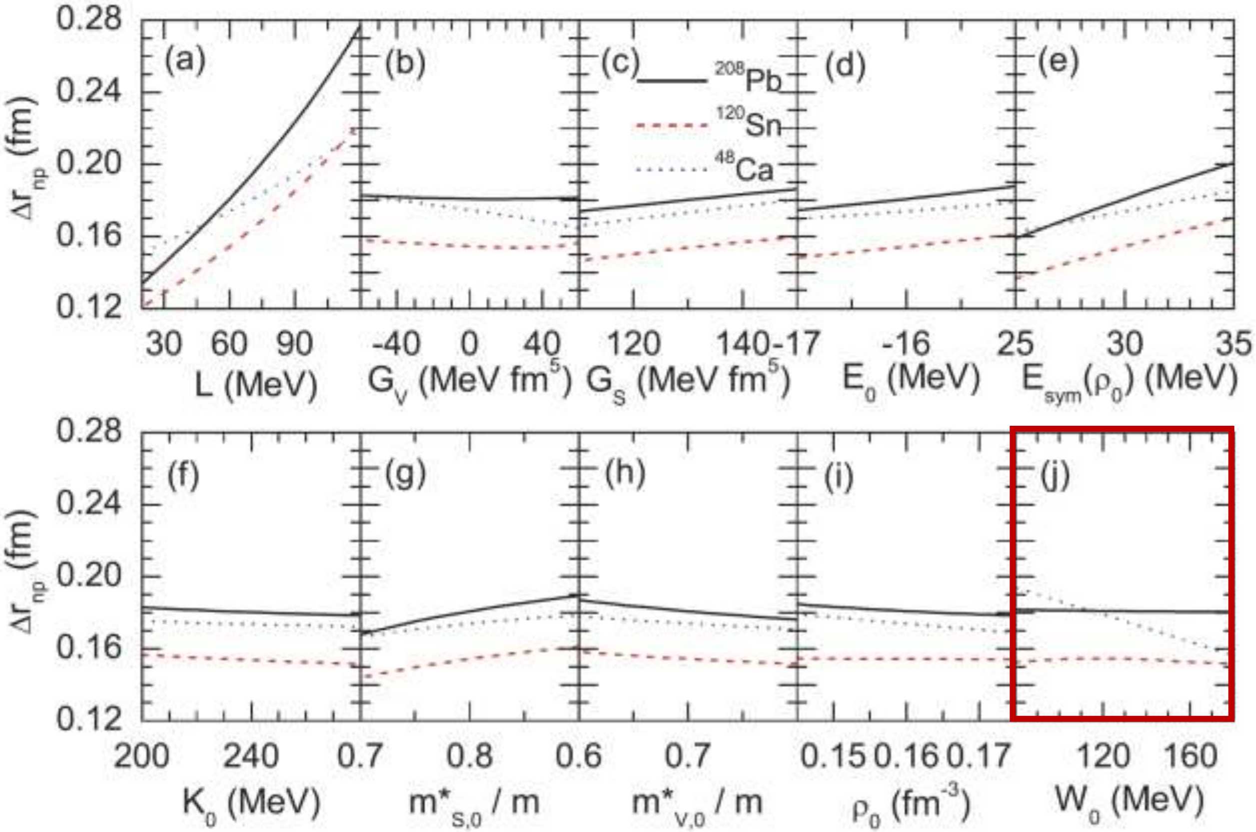

The Neutron skin of ^{48}Ca is sensitive to spin-orbit coupling W_0!

Chen, Ko, Li, &Xu, PRC82, 024321 (2010)

- ^{48}Ca and ^{208}Pb have different shell and surface structures
- Both are related to spin-orbit interaction

Nuclear spin-orbit interaction

Strong spin-orbit interaction→ magic numbers

$$U(r) \to U(r) + W(r) L \cdot S$$

Relativistic energy density functionals

$$W(r) = \frac{1}{2M^{*2} r} \frac{d(V - S)}{dr} L \cdot S$$

Duerr, Phys. Rev. 103, 469 (1956)

Mayer and Jensen (1949)

Nonrelativistic energy density functionals (Skyrme):

- Spin-orbit interaction: $iW_0 (\boldsymbol{\sigma}_1 + \boldsymbol{\sigma})_2 \cdot [\boldsymbol{P}' \times \delta(\boldsymbol{r}) \boldsymbol{P}]$

Chabanat, et al., NPA 627, 710 (1997)

- Spin-orbit energy: $E_{so} = \int dr^3 \frac{1}{2} W_0 [J \cdot \nabla\rho + J_p \nabla\rho_p + J_n \nabla\rho_n]$

$$= \int dr^3 \left[\frac{b_{IS}}{2} J \cdot \nabla\rho + \frac{b_{IV}}{2} (J_n - J_p) \nabla(\rho_n - \rho_p) \right]$$

Reinhard and Flocard, NPA 584, 467488 (1995)
Bender, Heenen, and Reinhard, Rev. Mod. Phys. 75, 121 (2003).
Ebran, Mutschler, Khan, and Vretenar, PRC 94, 024304 (2016).

- Standard Skyrme EDFs: Isoscalar dominant $b_{IV} = b_{IS}/3 = W_0/2$

Efforts in relativistic EDFs

- Meson-exchange relativistic mean field model
  - a) + tensor coupling.
  - b) + isoscalar-isovector mixing term in the scalar sector

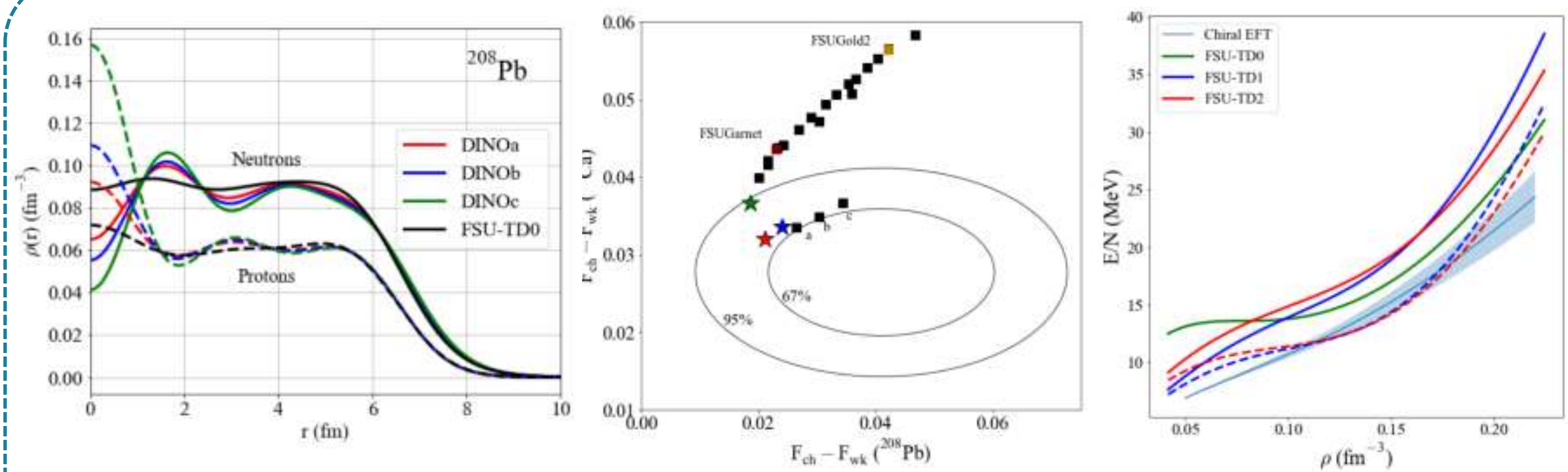

Salinas & Piekarewicz PRC109, 045807 (2024)

- Remove unphysical density oscillations.
- In slightly worse agreement with CREX and PREX
- In tension with Chiral EFT predictions for the neutron matter EOS